Impact of Thermal Cycling on Partial Discharge Inception Voltage in Random-Wound Electric Aircraft Motors

Anjana J. Samarakoon [1], Thomas F. Tallerico [2], Cameron Little [1],
Anubhav Bose [1], Aaron D. Anderson [2], Geoffrey Swisher [1], Kiruba Haran [1]
[1]Department of Electrical and Computer Engineering, University of Illinois Urbana Champaign, Urbana, Illinois, USA
Email: spa5@illinois.edu, clittle5@illinois.edu, bose15@illinois.edu, swisher5@illinois.edu, kharan@illinois.edu
[2]NASA Glenn Research Center, Cleveland, Ohio, USA
Email: thomas.tallerico@nasa.gov, aaron.d.anderson-1@nasa.gov

***Abstract*—Electric aircraft propulsion motors must simultaneously achieve high power density and reliability. To meet these requirements, electric aircraft motor winding insulation must maintain Partial Discharge (PD) free operation while experiencing significant thermal and electrical stresses throughout the operational lifetime. One of the primary stresses these motors will face is mechanical stress induced by thermal cycling, caused by take-off and landing mission cycles of the aircraft. This paper presents preliminary experimental results examining how Partial Discharge Inception Voltage (PDIV) is affected by these thermo-mechanical stress cycles. Motorette samples are prepared and subjected to various temperature cycles representative of an electric vertical takeoff and landing (eVTOL) vehicle application. PDIV measurements for turn-to-turn and phase-to-ground insulation are tracked over these temperature cycles. The PDIV behavior with the number of cycles and with different temperature profiles are investigated in this paper.**

***Index Terms*—electric propulsion, partial discharges, insulation reliability, thermal cycling, thermo-mechanical stresses.**

I. Introduction

Electric aircraft motors require insulation systems that enable high specific power and reliability. Conventional motor insulation rating systems define thermal classes based on constant temperature aging [1]–[3]. This system is insufficient for electric aircraft propulsion motors for two primary reasons. Firstly, it neglects the influence on the insulation system due to temperature cycling in electric aircraft motors [4]–[6]. Secondly, it rates insulation based on breakdown voltage criterion rather than the Partial Discharge Inception [3], [7], [8].

The electric motors used in aircraft and eVTOL propulsion applications operate with relatively short duty cycles. The motor windings heat up and cool down with each flight cycle and experience a corresponding thermo-mechanical stress cycle. Currently, for these conditions, a deterministic method for specifying the winding temperature limits and lifetime does not exist. Limited studies have been completed exploring the thermo-mechanical degradation of motor winding insulation [5], [9]–[13]. Madonna et al [14] completed a study on thermal cycle aging of motor coils for a UAM (Urban Air Mobility) application; however, their windings were not impregnated and correspondingly thermo-mechanical stress effects on the insulation were reduced. Their results did show the substantial benefit of physics of failure approaches to motor winding insulation ratings rather than relying on generic thermal class ratings.

The work presented in this paper explores the insulation degradation of impregnated random wound motor windings due to thermal cycles relevant to eVTOL applications. Impregnated random wound motor windings have three primary insulation systems: turn-to-turn, phase-to-ground, and phase-to-phase. At a minimum, one of these insulation systems (turn-to-turn) is expected to use Type-I (organic-based) insulation in electric aircraft motors because electric machines using Type-I insulation materials can deliver higher power densities compared to electric machines using Type-II insulation [15]. For inverter-fed Type-I insulation, the onset of partial discharge in the machine can be considered the end of life as Type-I insulation has very short lifetimes in the presence of partial discharge [16]. Correspondingly, aircraft motors must be designed to be PD-free for their lifetime. Therefore, this study tracks changes in the motor windings' PDIV with thermal cycles.

This paper presents preliminary experiments exploring the

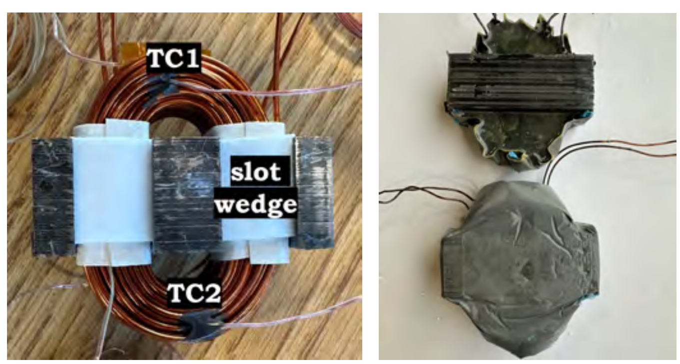

(a) (b)

Fig. 1: Motorette specimens (a) before impregnation and (b) after impregnation.

effects of thermo-mechanical aging on PDIV in motor windings under conditions representative of urban air mobility applications. Impregnated motorettes were manufactured and then thermal cycled repeatedly with different temperature profiles through joule heating of the windings. PDIV was measured for turn-to-turn and phase-to-ground insulation systems at different cycle counts. A similar previous study is presented in [4], but the PDIV data showed discrepancies, possibly due to defective specimens or defects in resin. Therefore, the work presented in this paper addresses those issues. All specimens are tested before impregnation and confirmed to be free of manufacturing defects, as described in II-A. Issues with specimens cracking in the curing process were addressed with a change in potting resin. Additionally, the PD measurement setup in this work has been improved over previous studies by incorporating a secondary PD detection method and minimizing the impact of electromagnetic interference (EMI).

The goal of this work is to create a dataset to guide future insulation aging model development and help develop design methodologies for high-reliability aircraft propulsion motors. The following sections present the experimental methodology and results.

II. Experimental Methodology

A. Specimens preparation

In this study, 10 motorette samples were prepared, each with a single coil wound around a single-tooth stator core, as shown in Fig. 1a. Each coil was wound with 16 AWG NEMA 1000 MW-16C magnet wires, selected for its high thermal class rating (240°C) suitable for high-power-density electric aircraft motors. The wound coils achieved approximately a 50% copper slot fill factor. To measure turn-to-turn PDIV degradation, each wound coil was formed by co-winding two wires to allow the application of electrical stress between them. The coils were all wound with approximately the same winding tension. A 0.08mm thick slot liner [17] was used as a part of the phase-to-ground insulation.

To ensure the specimens were defect-free prior to impregnation, the turn-to-turn and phase-to-ground PDIV of each coil was measured. The turn-to-turn PDIV measurements in each winding were compared against the turn-to-turn PDIV of twisted pair specimens made with same magnet wires according to IEC 60851-5 [18]. Table I shows the median turn-to-turn and phase-to-ground PDIV of five samples before the impregnation. The median turn-to-turn PDIV of the specimens was 608 V, while the measured median twisted-pair turn-to-turn PDIV was 612 V, confirming that the specimens were free of defects during fabrication.

TABLE I: Median PDIV values for unimgregnated specimens.

Specimen	Median Turn-to-Turn PDIV (V)	Median Phase-to-Ground PDIV (V)
1	608	1384
2	593	1434
3	608	1432
4	608	1419
5	595	1404

The samples then underwent vacuum pressure impregnation (VPI) process using a potting epoxy [19], selected for its high thermal conductivity and low coefficient of thermal expansion (CTE). A representative impregnated motorette is shown in Fig. 1b.

B. PD measurement setup

The PD measurement setup used in this study is shown in Fig. 2 and calibrated according to IEC-60270 standards [20]. For PDIV measurements, a 60 Hz sinusoidal voltage waveform was applied to the specimens. The voltage was

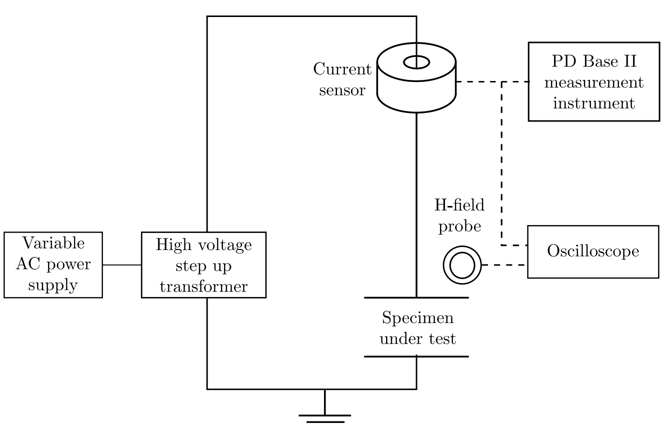

(a)

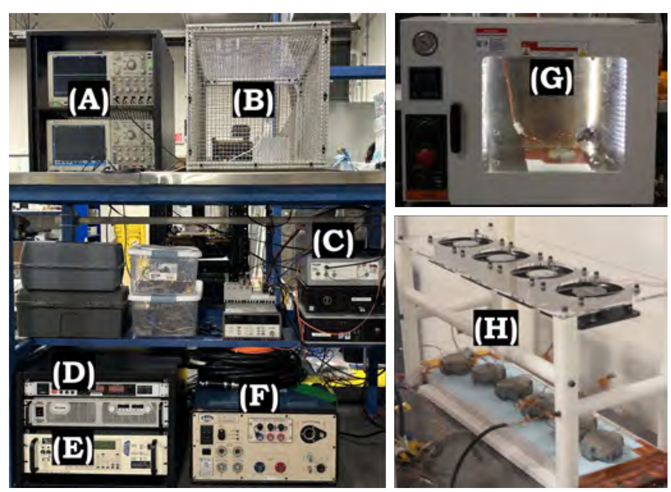

(b)

Fig. 2: PD test setup showing (a) the schematic and (b) instrumentation. The instruments are (A) oscilloscope (B) specimen test stand (C) PD Base II (D) high current supply for specimen aging (E) variable AC power supply (F) Doble M4100 high voltage insulation tester (G) vacuum oven for PD measurements at high temperature and vacuum (H) specimen aging setup.

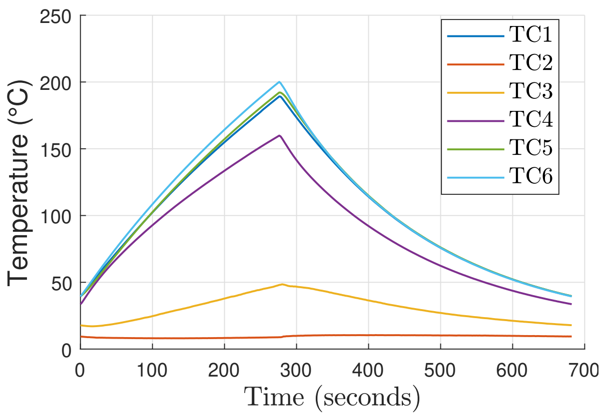

(a)

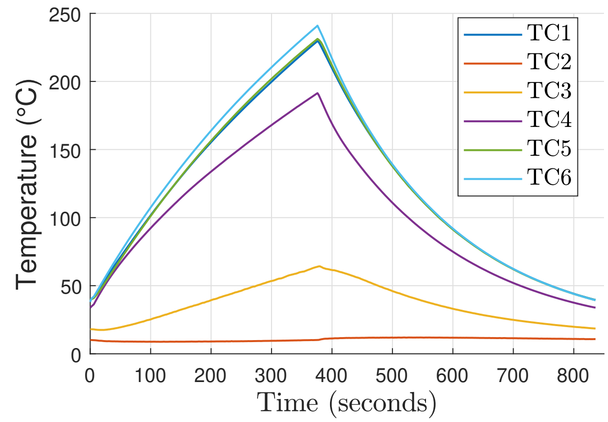

(b)

Fig. 3: Temperature distribution inside the motorette: (a) temperature profile with a peak temperature of 200°C, and (b) temperature profile with a peak temperature of 240°C. The thermocouple (TC) locations are: $TC1$ - slot wedge side of the winding, $TC2$ - cold plate surface, $TC3$ - side of the core as shown in Fig. 5, $TC4$ - inside the winding at the bottom of the slot, and $TC5$ & $TC6$ - end windings.

applied across the two co-wound magnet wires to measure turn-to-turn PDIV. Then, the turns were short-circuited, and voltage was applied between the magnet wires and the core to measure the phase-to-ground PDIV. The magnitude of the voltage waveform was increased at a rate of 3 Volts per second until PD was detected. PD was detected using a high-frequency current transformer (HFCT) and a magnetic field probe (H-probe) for redundancy. PDIV is defined in this paper as the voltage at which repetitive current pulses were detected. The threshold for PD was set to 100 pC. Five PDIV measurements were taken at each aging point for each sample.

PD measurements were taken at both ambient pressure and 0.2 atm. 0.2 atm was selected to match the pressure above 35,000 ft for fixed-wing aircraft applications. The PD measurement setup was tested and verified to be PD-free up to 2.8 kV at 1 atm. The vacuum PD setup, including the feedthroughs to the vacuum oven, was tested and verified to be PD-free up to 1.2 kV.

C. Aging with temperature cycles

The specimens were tested for PDIV after impregnation and were aged in groups of five. In electric propulsion motors, thermal cycles create mechanical stress in the motor winding insulation through the CTE mismatches of different materials and the thermal gradients through the motor stator. Both phase-to-ground and turn-to-turn are affected by the CTE mismatch, but phase-to-ground is often more impacted by thermal gradients between the core and the winding. The thermal aging setup was made to simulate both CTE mismatch and thermal gradient effects on the insulation. The thermal aging setup was made to emulate both of these effects. The samples were cycled on a cold plate, as shown Fig. 5. The cold plate was supplied with 5°C coolant to maintain a thermal gradient through the specimens and enable faster cooling portions of the thermal cycle. Heating of the windings to target temperatures was achieved by applying a constant current density ($20\,A/mm^2$), while thermocouples monitored the temperature. Each thermal cycle involved heating to a maximum temperature, cooling to 40°C, and then reapplying current until reaching the target cycle count.

The minimum peak winding temperature that would cause changes in PDIV was unknown. Therefore, for the first set of tests, the specimens were cycled between room temperature and progressively higher peak temperatures starting at 100°C. PDIV was measured after one thermal cycle and the test was repeated for peak temperatures 120, 140, 160, 180, and 200°C. 200°C was used as the upper limit as the epoxy glass transition is 205°C. No PDIV degradation was observed after any of these single cycles.

A set of five specimens were then cycled between 40°C and 200°C to study the PDIV degradation over higher cycle counts. The minimum temperature of 40°C was selected to reduce the cool-down times for the testing. A second set of five specimens was aged more aggressively with peak temperatures of 240°C. The temperature profiles from specimens that were instrumented with a number of thermal couples for both the 200°C and 240°C case are shown in Fig. 3a and 3b, respectively. As can be seen from both Fig. 3a and Fig. 3b, the hotspot temperature was measured at the end windings, and the temperature just under the slot wedge was within 10◦C from the end winding hotspot. However, the temperature of the core was 70°C or lower.

III. Results

Figures 4a, 4b, 4c show the measured minimum PDIV after different cycle counts for the turn-to-turn insulation at 1 atm and 0.2 atm, and the phase-to-ground insulation at 1 atm for specimens #1 through #5. These specimens were cycled at a peak temperature of 200°C. Similarly, Figures 4d, 4e, 4f show the measured minimum PDIV for the turn-to-turn insulation

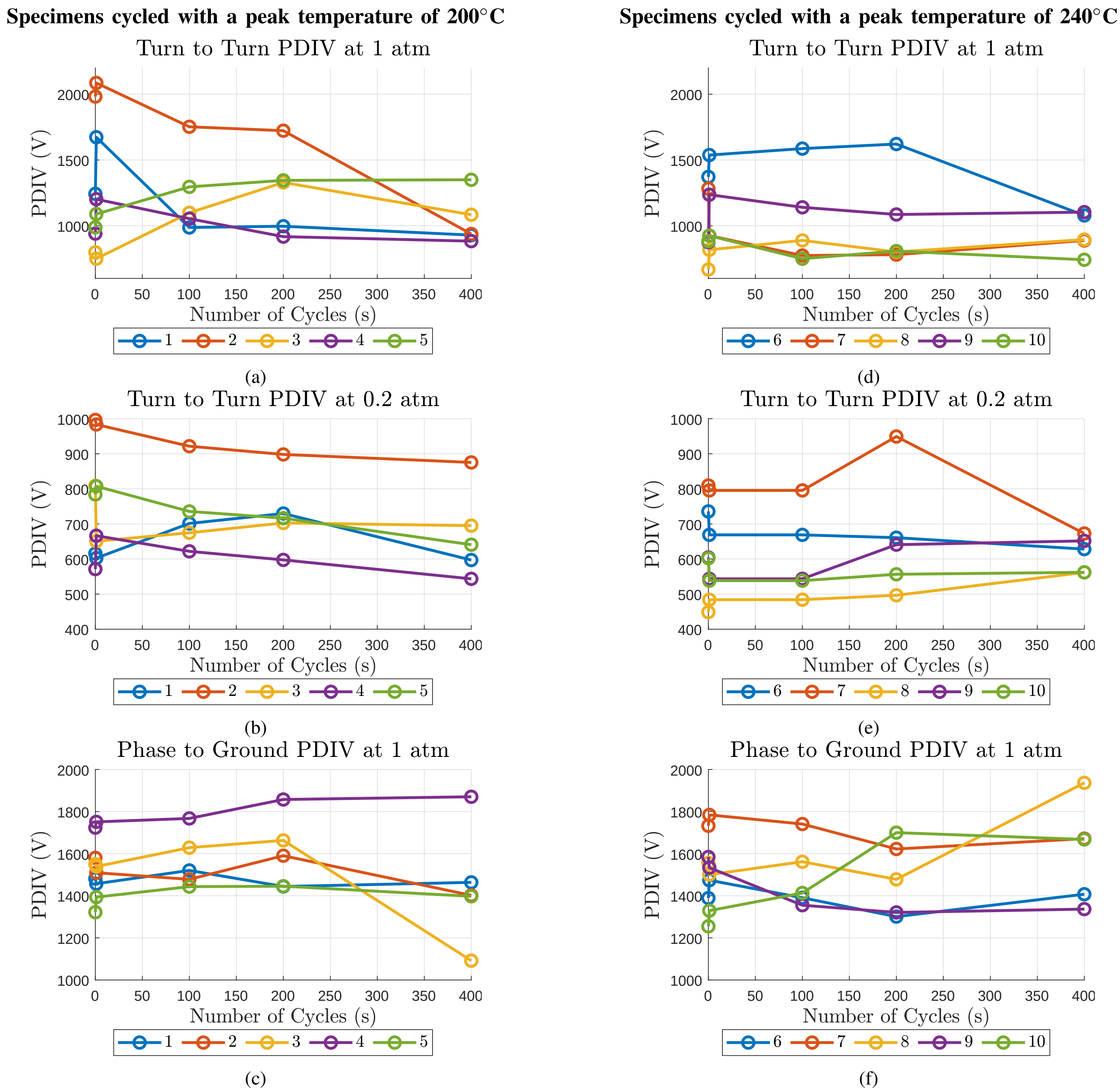

Fig. 4: Comparison of PDIV variation of different specimens aged under different thermal cycles.

at 1 atm and 0.2 atm, and the phase-to-ground insulation at 1 atm for specimens #6 through #10. These specimens were cycled at a peak temperature of 240°C.

IV. Discussion

Relative to the pre-impregnation measurements, the impregnation was able to increase the turn-to-turn PDIV of the random wound motorettes by an average of 1.2 to 3.3 times the unimpregnated or twisted pair turn-to-turn PDIV. The PDIV improvement of phase-to-ground insulation with impregnation was between 1.0 to 1.3 times the unimpregnated PDIV. The inconsistency in PDIV increase suggests some inconsistency in the manufacturing and potting process and a need to refine the process for future iterations.

According to Fig. 4a and Fig. 4b, turn-to-turn PDIV exhibits a generally gradual downward trend in PDIV against the number of cycles in specimens #1 through #5. Since these specimens were aged below the glass transition temperature of the resin, the degradation can be attributed to the thermally induced mechanical degradation. The highest degradation was in specimen #2, with a 50% turn-to-turn PDIV drop at 1 atm

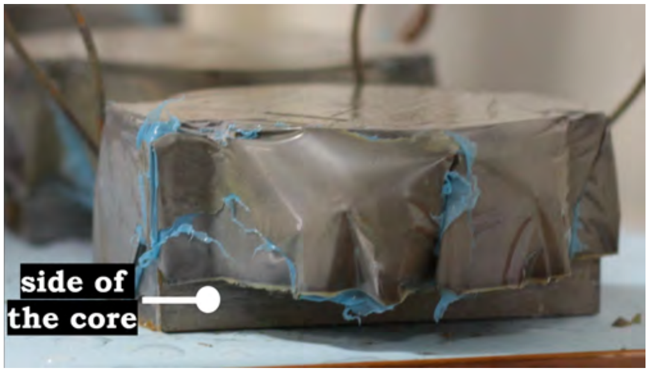

Fig. 5: Specimen showing the way it is placed on the cold plate and the location of measuring the core temperature.

after 400 cycles. The highest turn-to-turn PDIV degradation among specimens #6 through #10 was observed in specimen #7 with a 30% drop. Since these specimens were cycled with a peak temperature of 240°C, these specimens likely experienced some thermal-chemical aging of the epoxy in addition to thermo-mechanical aging.

While phase-to-ground PDIV of some specimens among specimens #1 through #10 exhibit a PDIV increase, there is a downward trend in most specimens. Although the specimens #6 through #10 reached a peak temperature of 240°C, the Nomex paper—the primary phase-to-ground insulation between the core and the winding—had a peak temperature below its rated datasheet temperature of 220°C. Therefore, this PDIV degradation can be attributed to the thermo-mechanical degradation.

V. Conclusion and Future Work

This paper presented preliminary experimental data of a study to understand the role of thermo-mechanical degradation on the PDIV of electric aircraft propulsion motor insulation. Tests were carried out below and above the epoxy thermal class limit but below the wire and slot liner insulation thermal class. The preliminary results show degradation in PDIV that can be attributed to thermal-mechanical cycling alone. Further thermal cycle testing of motorettes will help develop data and models for the design of PD-free insulation systems for electric aircraft applications.

VI. Acknowledgment

This work was supported by the National Science Foundation Engineering Research Center for Power Optimization of Electro-Thermal systems (POETS) with cooperative agreements EEC-1449548. The authors would like to acknowledge Dr. Andy Woodworth, Dr. Tim Krantz, and Dr. Mark Valco at NASA Glenn Research Center for directing this study and also helping to impregnate the motor winding samples with a high quality.

References

[1] ASTM, "ASTM D2307-2013 Standard Test Method for Thermal Endurance of Film-Insulated Round Magnet Wire," ASTM, 2013.

[2] T. Tallerico, A. D. Anderson, M. Hurrell, J. Gutknecht, M. Valco, and V. Sridhar, "Preliminary Measurements of Partial Discharge Inception Voltage Degradation with Constant Temperature Aging of Magnet Wire Twisted Pairs for Electric Aircraft Motors," 2024. [Online]. Available: http://www.sti.nasa.gov

[3] G. C. Stone, E. A. Boulter, I. Culbert, and H. Dhirani, *Electrical Insulation for Rotating Machines: Design, Evaluation, Aging, Testing, and Repair*, 2nd ed. John Wiley & Sons, 2014.

[4] A. J. Samarakoon, T. Tallerico, B. Wolhaupter, T. Balachandran, and K. Haran, "Partial discharge investigation of electric machine winding due to thermo-mechanical stresses for electric aircraft propulsion," in *2023 IEEE International Electric Machines Drives Conference (IEMDC)*, 2023, pp. 1–6.

[5] T. Tallerico, A. D. Anderson, M. Hurrell, J. Gutknecht, and M. Valco, "Initial Motor Winding Insulation Lifetime Experimental Results for Electric Aircraft Applications," *AIAA Aviation Forum and ASCEND, 2024*, 2024. [Online]. Available: https://arc.aiaa.org/doi/10.2514/6.2024-4100

[6] T. Tallerico, T. Krantz, M. Valco, and J. Salem, "Urban air mobility electric motor winding insulation reliability: Challenges in the design and qualification of high reliability electric motors and nasa's research plan," NASA, Cleveland, 2022.

[7] "Ieee standard test procedure for thermal evaluation of systems of insulating materials for random-wound ac electric machinery," *IEEE Std 117-2015 (Revision of IEEE Std 117-1974)*, pp. 1–34, 2016.

[8] "IEEE guide for the statistical analysis of thermal life test data," *ANSI/IEEE Std 101-1987(R2010) (Revision of IEEE Std 101-1972)*, pp. 1–34, 1988.

[9] Z. Huang, "Modeling and testing of insulation degradation due to dynamic thermal loading of electrical machines," Ph.D. dissertation, Lund University, 01 2017. [Online]. Available: https://lup.lub.lu.se/search/files/19894778/Binder1.pdf

[10] Z. Huang, A. Reinap, and M. Alaküla, "Degradation and fatigue of epoxy impregnated traction motors due to thermal and thermal induced mechanical stress - part i: Thermal mechanical simulation of single wire due to evenly distributed temperature," in *8th IET International Conference on Power Electronics, Machines and Drives (PEMD 2016)*, 2016, pp. 1–6.

[11] L. Yang, F. Pauli, and K. Hameyer, "Influence of thermal-mechanical stress on the insulation system of a low voltage electrical machine," *Archives of Electrical Engineering*, vol. 70, pp. 233–244, 2021.

[12] A. Griffo, I. Tsyokhla, and J. Wang, "Lifetime of machines undergoing thermal cycling stress," in *2019 IEEE Energy Conversion Congress and Exposition (ECCE)*, 2019, pp. 3831–3836.

[13] F. Loubeau, P. Rain, A. Durieux, and F. Le Strat, "Partial discharge behavior of motorettes under different aging conditions," in *2018 IEEE 2nd International Conference on Dielectrics (ICD)*, 2018, pp. 1–4.

[14] V. Madonna, P. Giangrande, and M. Galea, "Introducing physics of failure considerations in the electrical machines design," in *2019 IEEE International Electric Machines Drives Conference (IEMDC)*, 2019, pp. 2233–2238.

[15] T. Tallerico, T. Krantz, M. Valco, and J. Salem, "Urban Air Mobility Electric Motor Winding Insulation Reliability: Challenges in the Design and Qualification of High Reliability Electric Motors and NASA's Research Plan," 2022. [Online]. Available: http://www.sti.nasa.gov

[16] V. Madonna, P. Giangrande, W. Zhao, H. Zhang, C. Gerada, and M. Galea, "Electrical machines for the more electric aircraft: Partial discharges investigation," *IEEE Transactions on Industry Applications*, vol. 57, no. 2, pp. 1389–1398, 2021.

[17] DuPont, "Nomex type 414 datasheet," 2025, accessed: Mar. 23, 2025. [Online]. Available: https://www.dupont.com/content/dam/dupont/amer/us/en/safety/public/documents/en/Nomex-Type-414.pdf

[18] International Electrotechnical Commission, "IEC 60851-5: Winding wires - Test methods - Part 5: Electrical properties," 2021, accessed: Mar. 23, 2025. [Online]. Available: https://webstore.iec.ch/en/publication/65757

[19] Parker Hannifin Corporation, "CoolTherm EP-2000 Datasheet," 2023, available online: https://www.parker.com/content/dam/Parker-com/Literature/Assembly---Protection-Solutions-Division/Technical-Datasheets-(TDS)/Datasheet---CoolThermEP-2000(EnglishA4)_DS4323E.pdf.

[20] International Electrotechnical Commission, "IEC 60270:2000 - High-voltage test techniques - Partial discharge measurements," 2000, available online: {https://webstore.iec.ch/en/publication/1247.